Impact of the Structural Changes on the Attenuation Properties of some Nickel Borate-Based Glasses Containing Lead and Lanthanum Cations for Gamma-ray Shielding Applications

Sarah M. Kamil[1*], *Ashraf. A. Abul-Magd*[2], *W. El-Gammal*[3], *H. A. Saudi*[4]

[1] National Institute for Standards, Giza, Egypt.
[2] Basic Science Department, Faculty of Engineering, Sinai University, El-Arish, Egypt.
[3] Egyptian Nuclear and Radiological Regulatory Authority, Cairo, Egypt.
[4] Department of Physics, Faculty of Science, Al-Azhar University, (Girls' Branch), Cairo, Egypt.

Abstract: Some of the nickel borate-based glasses, containing lead and lanthanum cations as gamma-ray shielding, were prepared using traditional melting method. XRD patterns confirm the non-crystallinity of the samples. According to FTIR, with lead entering the structural network, the structural groups of BO_4 and PbO_4 increased, and the structural network became more stable and able to absorb gamma rays. Theoretical studies showed agreement with the experimental, and the attenuation parameters of these samples proved that they are capable of absorbing gamma rays with a thickness lighter than ordinary concrete.

Keywords: Oxide glass, Density, FTIR, Shielding, X-Com.

1 Introduction

With the increased use of gamma-ray active isotopes in industry, medicine, and agriculture, it has become necessary to investigate the shielding ability in a variety of materials of technological and biological importance [1], [2]. Shielding materials for nuclear radiation situations must be continuously developed [2]. This is because shielding materials are so large that a detailed understanding of radiation flux propagation in shielding materials is required for shield design. For example, in order to calculate the attenuation coefficients, the water content in concrete layers must be taken into account. Concrete layers are also opaque to visible light, which adds further uncertainty to the attenuation coefficient calculations. This has been made possible by the invention of theoretical tables and a computer software (XCOM) for calculating mass attenuation coefficients [3], [4].

It is important that the material used in shield design be homogeneous in terms of density and composition. Glass is one of the most promising materials for use as radiation shields because of qualities such as ease of preparation, light transparency, and doping ability, which allow it to become an excellent absorbing material [5]. Glass is a

transparent shielding material that can be improved by using heavy elements like Mo, Bi, La, and Pb. Medical rooms, X-ray facilities, nuclear research centers, and other institutions that employ radiation can all benefit from using glass shields [6]. Many manufacturers have studied glass such as Si and B for their optical and shielding qualities, and nuclear engineers have created a variety of glasses that enable vision while also absorbing radiation such as gamma rays and neutrons, such as adding heavy metal oxides (HMO) to the glass, and this enhances the attenuation effectiveness of the glass matrix [5]. Lanthanum oxide glasses have very high refractive indices and low dispersion. These eyeglasses are used in complex lenses for cameras, binoculars and military instruments for the purpose of correcting spherical and chromatic aberrations. Rare-earth oxides are often added to molten glass in order to produce special glass [7].

Certain research have recently addressed the effect of nickel oxide additions to a range of modified borate glasses [8]–[11], where they verified the existence of Ni ions in borate glasses as a network former. More than one valence state in borate glasses doped with transition metal ions gives them excellent optical and electrical characteristics [9], [10]. Radiation shielding [9], [12], solar collectors, broadband amplifiers, phosphors, and tunable lasers [8], [10] have all seen increased interest in NiO doping with modified borate glasses.

---

*Corresponding author e-mail: sar3y@yahoo.com

The purpose of this work is to prepare the glass compound PbO - B_2O_3 - La_2O_3 - NiO as gamma-ray protective shields. X-ray and FTIR were used to investigate the composition. The attenuation parameters will calculate theoretically and compare them with practical measurements.

2 Experimental Procedures:

Lanthanum Nickel Lead Borate glasses of compositions 80 B_2O_3– 4 La_2O_3– (12+x) PbO –(4-x) NiO, (x = 0,1,2,3 or 4) were set up by melt quenching method. The stoichiometric quantities of nickel oxide, lanthanum oxide, boric acid, lead monoxide is completely blended and structured in porcelain crucibles. The samples were placed in the oven at room temperature, then gradually increased to 1200°C. The samples were melted for about two hours until a bubble-free liquid formed, and the melt was occasionally properly mixed. The resultant dissolve was immediately poured into two treating steel sheets and tightened to 300 ^{o}C in order to eliminate warm strains. The creation of the glass tests utilized in the current examination is arranged in Table (1).

Table 1: Chemical compositions of [80 B_2O_3– 4 La_2O_3– (12+x) PbO –(4-x) NiO].

Sample code	Composition mole fraction (mol %)			
	B_2O_3	La_2O	PbO	NiO
Pb12	80	4	12	4
Pb13	80	4	13	3
Pb14	80	4	14	2
Pb15	80	4	15	1
Pb16	80	4	16	0

The case of amorphous glass was examined by the method of X-ray diffraction, using Philips PW (1140) diffractometer at RT with copper target (K_a=1.54 A^o). For several glass samples, KBr pellet technique was used on a Perkin–Elmer 467 IR spectrometer to create the vibration spectra from 400 to 4000 cm^{-1}. The standard Archimedes principle was used to determine the densities of the glass samples. These data were determined utilizing a single pan balance and xylene as an inundation liquid. ^{60}Co and ^{137}Cs (10 µCi) point sources were used to excite the targets (show Figure 1). Gamma-ray intensity was measured using NaI (Tl) 2 × 2 scintillation detector. The mass attenuation coefficient (MAC) which indicates how easily gamma rays can penetrate a certain material and given by [1], [13] :

$$MAC_= \mu_L/\rho \qquad (1)$$

where, μ_L is the linear attenuation coefficient and ρ is the material density. μ_L is calculated from Beer–Lambert law of formula [14]:

$$I = I_0 \, e^{-\mu_L.x} \qquad (2)$$

where, x is the distance, over which the attenuation takes place. By Knowing μ_L the mean free path (MFP) can be calculated which is the average distance travelled by a photon between collisions (MFP = 1/ μ_L). Half value layer (HVL) is the thickness of the material in which half of the radiation has been attenuated (HVL= Ln (2) / μ_L). The active atomic number (Z_{eff}) plays a major role in the evaluation of the energy-related variable as an alternative material. The interaction such as gamma ray absorption depend on the Z_{eff} of the composite and the photon energy. Generally high Z_{eff} materials are powerful absorbing material. The Z_{eff} can be calculated using the following formula [13]. We can calculate the Z_{eff} with the following:

$$Z_{eff} = \frac{\sum_i f_i A_i (\frac{\mu}{\rho})_i}{\sum_i f_i \frac{A_i}{Z_i}(\frac{\mu}{\rho})_i} \qquad (3)$$

where, each constituent element, f_i represent the mole fraction, A_i the atomic weight and Z_i the atomic number of the i*th* constituent element, respectively. Energy-dependent effective electron density (N_{eff}). is also calculated as follows:

$$N_{eff} = \frac{Z_{eff} N_A \sum_i n_i}{\sum_i f_i A_i} \qquad (4)$$

where Σn_i is the total number of elements in the material[13].
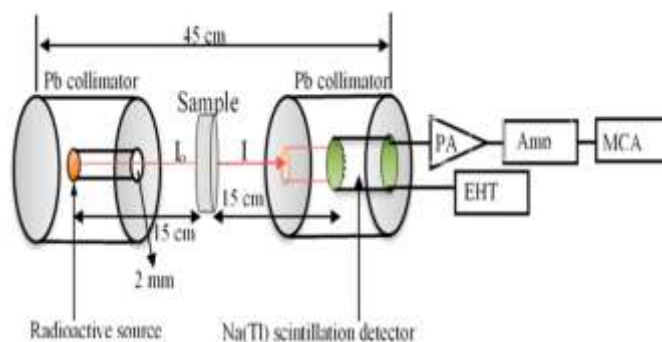
Fig. 1: Radiation measurements setup.

3 Results and Discussion

3.1 XRD Analysis and Density Measurements

The X-ray diffraction (XRD) profiles of both 12.0 and 16.0 percent mol PbO are shown in Figure 2. The current samples can be described as a glassy (amorphous) material. Amorphous materials' behavior is characterized by the absence of sharp peaks and the presence of only two wide edges in each sample[15].

Figure 3 shows that the density of the examined glass samples increases as the amount of lead oxide increases. Because the density of NiO (6.67 g/cm^3) is much lower than that of PbO (9.53 g/cm^3) in the samples under

investigation, this behavior appears logical.
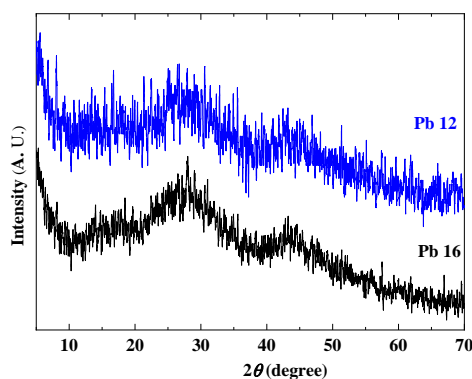
Fig. 2: XRD Charts for 12.0 and 16.0 % mol PbO.
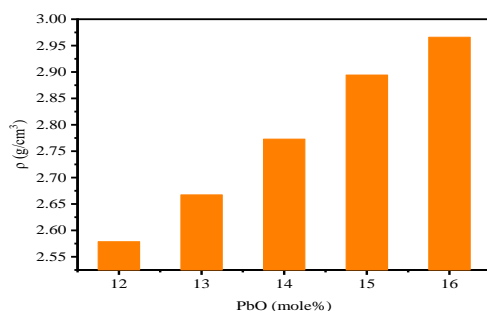
Fig.3: Variety of density of Lanthanum Nickel Lead Borate glasses with the PbO content.

3.2 FTIR Measurement:

In order to explore and study the structure of a material, an FTIR spectrometer is an important tool in material research. The infrared spectrum has the ability to identify molecules and provide comprehensive information on the presence or absence of functional groups in a substance [16]. The FTIR spectrum of the present glassy system is shown in Figure 4. The absorbed bands in the first spectral range (400-600 cm^{-1}) are responsible for metal cation vibration and particular deformation patterns [16] Within this range, two weak bands with varying intensities are detected at 454 and 542 cm^{-1}; the first is typically attributed to the PbO symmetric expansion vibration bonds in PbO_4 and/or the LaO_6 metallic vibrations [17], while the second is attributed to particular Ni–O and La–O bonds [12]. The intensity of these two bands varied depending on the amount of PbO present, which reflects the role of Ni^+ ions in breaking down the bonds that form the lattice and also explains the role of Pb ions in making Pb-O connections, where it is clear that Pb ions enter the reticular structure of the samples, causing a change in the network structure.

It has been determined that B–O–B bending vibrations

are responsible for the bands between 600 and 800 cm^{-1}. BO_4 unit stretching vibrations are responsible for the absorption bands between 800 and 1200 cm^1 [18][19][15]. B–O stretching vibrations of trigonal BO_3 units cause absorption bands in the 1200-1600 cm^{-1} range [19][20] [21]. There are bending vibrations in the H–O–H system that are responsible for the absorption bands at 1640 cm^{-1} [22]. With the addition of PbO, the intensity of the BO_3 vibration band grew, suggesting the replacement of trigonal units (BO_3) by tetrahedral (BO_4) units, and decreased non-bridle oxygens (NBO's), at the cost of Ni^+ ions, reflecting structural changes caused by Pb^+ ions entrance.
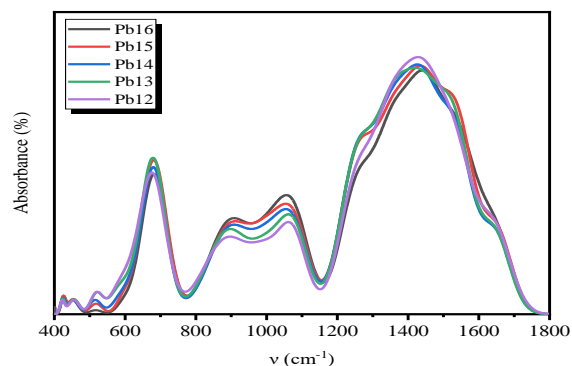
Fig. 4: FTIR spectrum of the investigated materials.
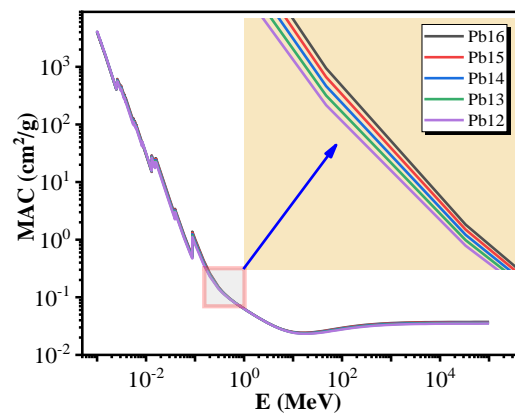
Fig. 5: MAC of glass samples vs. incident photon energy.

3.3 Gamma Radiation Shielding Characterizations

The shielding qualities of the glass samples were verified using Microsoft XCOM software to determine mass attenuation coefficients (MAC) at different photon energies[23], which were also measured experimentally. The theoretical results computed using the XCOM program at various gamma ray energies and PbO concentrations are plotted and presented in Figure 5. The onset graph in Figure 5 shows that MAC has a high energy dependence in the low

energy region, where it decreases rapidly with increasing energy photon for all samples. They do, however, demonstrate a weak energy dependence at higher energies. Because the method of interaction between gamma-rays and matter is dependent on the energy of the incident photon, this can be clarified. The photoelectric effect dominates at low energies, but Compton scattering and pair production dominate at higher energies. Figures 6, 7 show the change of theoretical and experimental MAC in contrast to conventional concrete at 0.356 MeV and 0.662 MeV, respectively. The experimental and theoretical values are in good agreement. The increase in MAC with increasing PbO concentrations can be explained by the fact that PbO has a higher absorption coefficient than NiO, and that lead has entered the lattice structure of the samples, resulting in a higher absorption for lead, as well as an increase in the density of glass samples with increasing PbO content. At both energies of 0.356 MeV and 0.662 MeV, the MAC value for all PbO ratios in Lanthanum Nickel Lead Borate glasses is greater than that of ordinary concrete. Figures 8, 9 depicts the half value layer (HVL) of the present glasses and its variation across gamma ray energy and PbO mol percent concentrations at 0.356 MeV and 0.662 MeV respectively.
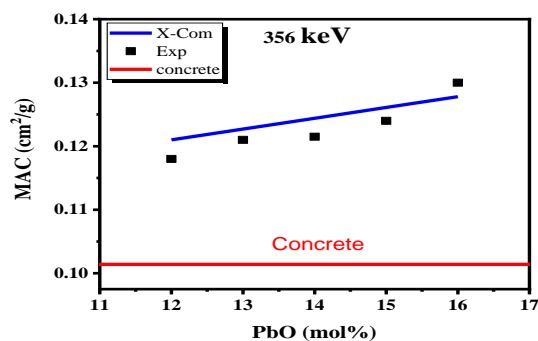
Fig. 6: Experimental and theoretical MAC vs PbO ratio in the glass system at 356 kev, as well as the concrete MAC value.
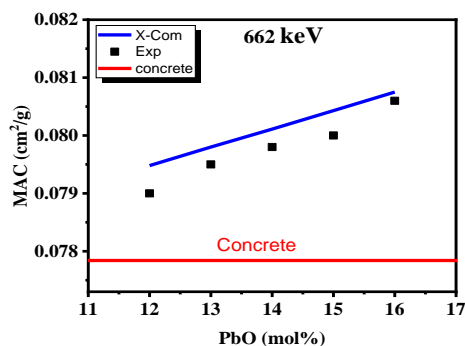
Fig. 7: Experimental and theoretical MAC vs PbO ratio in the glass system at 662 kev, as well as the concrete MAC value.
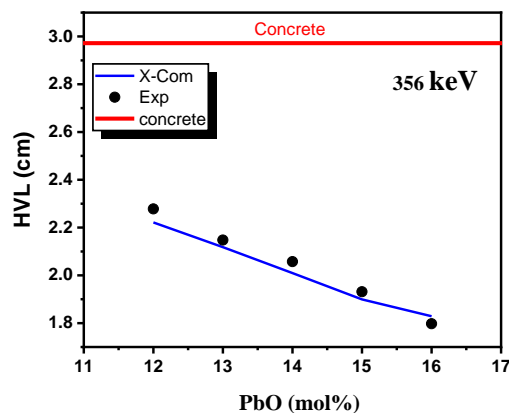
Fig.8: Concrete HVL value as well as experimental and theoretical HVL vs PbO ratio in samples at 356 keV.
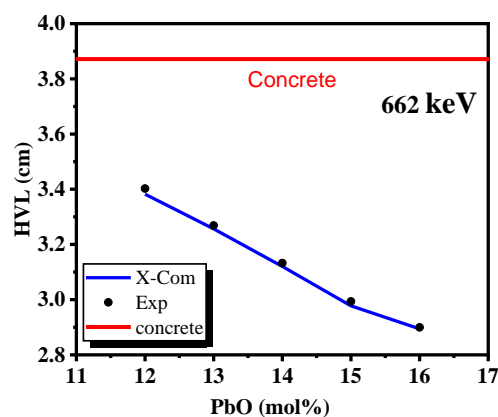
Fig. 9: Concrete HVL value as well as experimental and theoretical HVL vs PbO ratio in samples at 662 kev.

According to Figures 8, 9 the HVL values drop as the PbO level increases. Lower HVL values indicate that the material has a greater ability to interact with the incident gamma ray photon, which is a good thing. It is reported that the sample with the highest percentage of lead Pb16 is the best sample that has been prepared, as it has the lowest HVL, the highest mass attenuation coefficient, and the highest density, indicating that it has better shielding properties. As shown in Figure 10, the MFP increase by increasing the photon energy and by decreasing PbO ratio as the sample's density decrease. The sample Pb16 gives the smallest MFP.

For all prepared glass samples both Z_{eff} values decrease with increasing photon energy. Figure 11 illustrates that the values of Z_{eff} increase along with PbO concentration for different energies of gamma radiation. Z_{eff} has a high energy dependence in the low energy region, where it decreases rapidly with increasing energy photon for all samples, which approximately shows the same behavior to that of MAC as a function of energy and concentration of PbO.
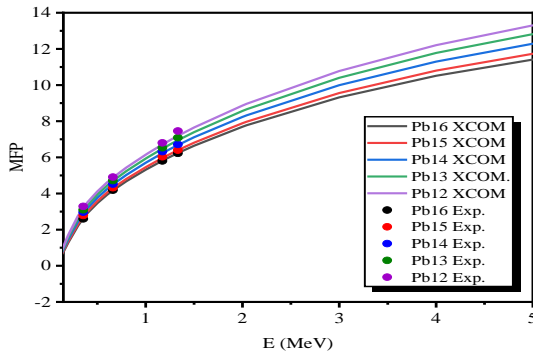
Fig. 10: MFP of glass samples vs. photon energy.
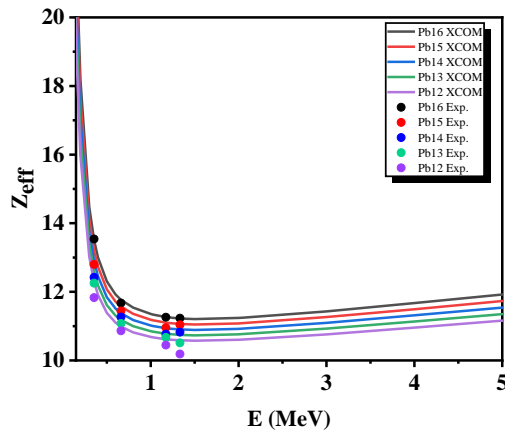
Fig.11: Z_{eff} of glass samples vs. incident photon energy.
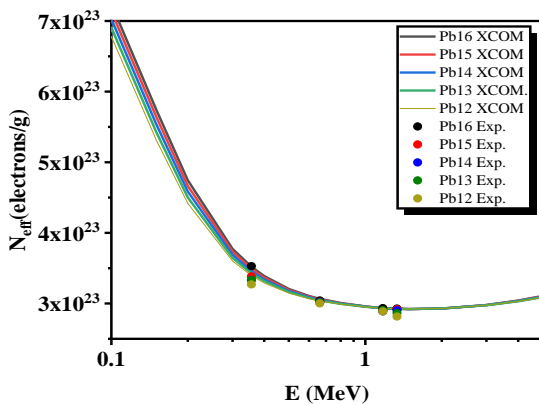
Fig. 12: N_{eff} of glass samples vs. incident photon energy.

Figure 12 indicates the values of N_{eff} it is seen that the formation of free electrons in the region dominated by photoelectric absorption is higher than in other regions. Because the photons in this region have low energies and higher wavelengths, they are more likely to interact with target material electrons. This high probability leads to more photon absorption by electrons, resulting in more free electrons. illustrates that the values of N_{eff} decrease by

increasing of the photon energy for all PbO concentration increase, the Pb16 sample had the highest N_{eff} value.

4 Conclusions

Glass samples were prepared from [B_2O_3– La_2O_3– PbO– NiO], which are transparent to visible light. X-rays were used to confirm the amorphous condition of the glass. MAC, HVL, MFP, and Z_{eff}, were determined in order to understand the photon attenuation abilities of the studied samples. It can be concluded that MAC and Z_{eff} values increase as PbO percent increases. In addition, they decrease exponentially as the gamma ray photon energy increases. On the other hand, HVL and MFP values decrease as the PbO percent increases. There was good agreement between the experimental results and theoretical calculations the present work. This composition of glass could absorb gamma rays with a thickness lighter and less than ordinary concrete when compared, as it has higher MAC value, lower HVL and MFP than ordinary concrete

The results proved that the mass attenuation coefficient is high and the HVL is low, which proves that this composition of glass could absorb gamma rays with a thickness lighter and less than ordinary concrete when compared. FTIR revealed that lead entered the vitreous structure of the samples, which contributed to the higher gamma absorption. Also, the intensity and absorption of gamma rays increase with the increase in the percentage of lead, and therefore 16 Pb is the one that we recommend using as a shield, especially at low gamma radiation energy.

References

[1] A. M. Zoulfakar, A. M. Abdel-Ghany, T. Z. Abou-Elnasr, A. G. Mostafa, S. M. Salem, and H. H. El-Bahnaswy, "Effect of antimony-oxide on the shielding properties of some sodium-boro-silicate glasses," *Applied Radiation and Isotopes*., **127**., 269–274, 2017, doi: 10.1016/j.apradiso.2017.05.007.

[2] N. Singh, K. J. Singh, K. Singh, and H. Singh, "Comparative study of lead borate and bismuth lead borate glass systems as gamma-radiation shielding materials," *Nucl. Instruments Methods Phys. Res. Sect. B Beam Interact. with Mater. Atoms*., **225(3)**, 305–309, 2004, doi: 10.1016/j.nimb.2004.05.016.

[3] H. A. Saudi and S. U. El-Kameesy, "Investigation of modified zinc borate glasses doped with BaO as a nuclear radiation-shielding material," *Radiat. Detect. Technol. Methods*., **2(2)**, 1–7, 2018, doi: 10.1007/s41605-018-0075-x.

[4] H. A. Saudi, A. G. Mostafa, N. Sheta, S. U. El Kameesy, and H. A. Sallam, "The structural properties of CdOBi2O3 borophosphate glass system containing Fe2O3 and its role in attenuating neutrons and gamma rays," *Physica B: Condensed Matter*., **406(21)**, 4001–4006, 2011, doi: 10.1016/j.physb.2011.06.038.

[5] Y. Al-Hadeethi and M. I. Sayyed, "BaO–Li2O–B2O3 glass systems: Potential utilization in gamma radiation protection," *Prog. Nucl. Energy*., **129**(no. September), p. 103511, 2020, doi: 10.1016/j.pnucene.2020.103511.

[6] Y. Al-Hadeethi, M. I. Sayyed, and Y. S. Rammah, "Fabrication, optical, structural and gamma radiation shielding characterizations of GeO2-PbO-Al2O3–CaO glasses," *Ceram. Int.*, **46(2)**, 2055–2062, 2020, doi: 10.1016/j.ceramint.2019.09.185.

[7] A. El-Taher, "Nuclear Analytical Techniques for Detection of Rare Earth Elements," *J. Radiat. Nucl. Appl.*, **3(1)**, 53–64, 2018, doi: 10.18576/jrna/030107.

[8] P. V. Rao, G. N. Raju, P. S. Prasad, C. Laxmikanth, and N. Veeraiah, "Transport and spectroscopic properties of nickel ions in ZnO-B2O3-P2O5 glass system," *Optik (Stuttg).*, **127(5)**, 2920–2923, 2016, doi: 10.1016/j.ijleo.2015.12.056.

[9] R. M. El-Sharkawy, K. S. Shaaban, R. Elsaman, E. A. Allam, A. El-Taher, and M. E. Mahmoud, "Investigation of mechanical and radiation shielding characteristics of novel glass systems with the composition xNiO-20ZnO-60B2O3-(20-x) CdO based on nanometal oxides," *J. Non. Cryst. Solids*, ., **528**, no. October,119754, 2020, doi: 10.1016/j.jnoncrysol.2019.119754.

[10] S. Thakur, V. Thakur, A. Kaur, and L. Singh, "Structural, optical and thermal properties of nickel doped bismuth borate glasses," *J. Non. Cryst. Solids*, vol. 512, no. January., 60–71, 2019, doi: 10.1016/j.jnoncrysol.2019.02.012.

[11] S. Suresh, T. Narendrudu, A. S. Kumar, M. V. S. Rao, G. C. Ram, and D. K. Rao, "Role of nickel ion coordination on spectroscopic properties of multi-component CaF2–Bi2O3–P2O5–B2O3 glass-ceramics," *Opt. Mater. (Amst).*, **60**, 67–73, 2016, doi: 10.1016/j.optmat.2016.07.012.

[12] A. A. Abul-Magd, H. Y. Morshidy, and A. M. Abdel-Ghany, "The role of NiO on the structural and optical properties of sodium zinc borate glasses," *Opt. Mater. (Amst).*, vol. 109, no. June, 110301, 2020, doi: 10.1016/j.optmat.2020.110301.

[13] B. ALIM, "Determination of Radiation Protection Features of the Ag2O Doped Boro-Tellurite Glasses Using Phy-X / PSD Software," *J. Inst. Sci. Technol.*, **10(1)**, 202–213, 2020, doi: 10.21597/jist.640027.

[14] H. M. Mahmoud, A. S. Hok, E. Armia, and A. El-Taher, "Gamma-ray absorption and scattering coefficients for two sedimentary rocks," *Indian J. Pure Appl. Phys.*, **33**, no. June 1995, 332–344, 1995.

[15] Y. B. Saddeek, K. H. S. Shaaban, R. Elsaman, A. El-Taher, and T. Z. Amer, "Attenuation-density anomalous relationship of lead alkali borosilicate glasses," *Radiat. Phys. Chem.*,. **150**, 182–188, 2018, doi: 10.1016/j.radphyschem.2018.04.028.

[16] S. M. Kamil and H. M. Gomaa, "Effect of exchanging PbO with NiO on the structure and optical parameters action of some lanthanum borate oxide glasses," *J. Mater. Sci. Mater. Electron.*, 2021, doi: 10.1007/s10854-021-06882-7.

[17] K. S. Shaaban, M. S. I. Koubisy, H. Y. Zahran, and I. S. Yahia, "Spectroscopic Properties, Electronic Polarizability, and Optical Basicity of Titanium–Cadmium Tellurite Glasses Doped with Different Amounts of Lanthanum," *J. Inorg. Organomet. Polym. Mater.*, **30(12)**, 4999–5008, 2020, doi: 10.1007/s10904-020-01640-4.

[18] E. A. Elkelany, M. A. Hassan, A. Samir, A. M. Abdel-Ghany, H. H. El-Bahnasawy, and M. Farouk, "Optical and Mössbauer spectroscopy of lithium tetraborate glass doped with iron oxide," *Optical Materials*., 112. 2021, doi: 10.1016/j.optmat.2020.110744.

[19] HMH Zakaly, A Ashry, A. El-Taher, AGE Abbady, Elhassan A Allam, Rehab M El-Sharkawy, Mohamed E Mahmoud., Role of novel ternary nanocomposites polypropylene in nuclear radiation attenuation properties: In-depth simulation study. Radiation Physics and Chemistry 188, 109667.2021.

[20] S. Mitrici *et al.*, "Nickel-lead-borate glasses and vitroceramics with antiferromagnetic NiO and nickel-orthoborate crystalline phases," *J. Non. Cryst. Solids*, **471**, no. June, 349–356, 2017, doi: 10.1016/j.jnoncrysol.2017.06.019.

[21] A El-Taher, HMH Zakaly, M Pyshkina, EA Allam, RM El-Sharkawy, Mohamed E Mahmoud, Mohamed AE Abdel-Rahman A comparative Study Between Fluka and Microshield Modeling Calculations to study the Radiation-Shielding of Nanoparticles and Plastic Waste composites. Zeitschrift für anorganische und allgemeine Chemie., **647 (10)**, 1083-1090, 2021.

[22] A. S. Abouhaswa, Y. S. Rammah, M. I. Sayyed, and H. O. Tekin, "Synthesis, structure, optical and gamma radiation shielding properties of B2O3-PbO2-Bi2O3 glasses," *Compos. Part B Eng.*, vol. 172, no. March., 218–225, 2019, doi: 10.1016/j.compositesb.2019.05.040.

[23] M. E. Mahmoud, R. M.El-Sharkawy, E. A. Allam, R. Elsaman, and A. El-Taher, "Fabrication and characterization of phosphotungstic acid - Copper oxide nanoparticles - Plastic waste nanocomposites for enhanced radiation-shielding," *J. Alloys Compd.*, **803**, 768–777, 2019, doi: 10.1016/j.jallcom.2019.06.290.